nature COMMUNICATIONS

ARTICLE

Received 4 Sep 2014 | Accepted 20 Jan 2015 | Published 6 Mar 2015

DOI: 10.1038/ncomms7338

Two linked pairs of *Arabidopsis TNL* resistance genes independently confer recognition of bacterial effector AvrRps4

Simon B. Saucet[1,*], Yan Ma[1,*], Panagiotis F. Sarris[1], Oliver J. Furzer[1], Kee Hoon Sohn[2] & Jonathan D.G. Jones[1]

Plant immunity requires recognition of pathogen effectors by intracellular NB-LRR immune receptors encoded by *Resistance* (*R*) genes. Most R proteins recognize a specific effector, but some function in pairs that recognize multiple effectors. *Arabidopsis thaliana* TIR-NB-LRR proteins RRS1-R and RPS4 together recognize two bacterial effectors, AvrRps4 from *Pseudomonas syringae* and PopP2 from *Ralstonia solanacearum*. However, AvrRps4, but not PopP2, is recognized in *rrs1/rps4* mutants. We reveal an *R* gene pair that resembles and is linked to *RRS1/RPS4*, designated as *RRS1B/RPS4B*, which confers recognition of AvrRps4 but not PopP2. Like RRS1/RPS4, RRS1B/RPS4B proteins associate and activate defence genes upon AvrRps4 recognition. Inappropriate combinations (RRS1/RPS4B or RRS1B/RPS4) are non-functional and this specificity is not TIR domain dependent. Distinct putative orthologues of both pairs are maintained in the genomes of *Arabidopsis thaliana* relatives and are likely derived from a common ancestor pair. Our results provide novel insights into paired *R* gene function and evolution.

[1] Sainsbury Laboratory, Norwich Research Park, Norwich NR4 7UH, UK. [2] Bioprotection Research Centre, Institute of Agriculture and Environment, Massey University, Private Bag 11222, Palmerston North 4442, New Zealand. * These authors contributed equally to this work. Correspondence and requests for materials should be addressed to J.D.G.J. (email: jonathan.jones@tsl.ac.uk).

Plant immunity is activated upon direct or indirect perception of pathogen molecules. Cell surface receptors perceive relatively invariant pathogen molecules such as flagellin or chitin, and intracellular receptors perceive the presence or action of pathogen effectors[1]. The intracellular immune receptors are called resistance (R) proteins and encoded by *R* genes. Effector recognition by R proteins leads to effector-triggered immunity, which often culminates in programmed cell death, also known as the hypersensitive response (HR)[2]. However, disease resistance can be achieved without HR[3]. Most plant *R* genes encode nucleotide-binding, leucine-rich repeat (NB-LRR) proteins that structurally and functionally resemble mammalian nucleotide-oligomerization domain-like (NOD-like) receptors[4]. NB-LRR proteins are modular and presumed to undergo intra- and inter-molecular reconfiguration upon effector recognition, activating defence[5]. However, mechanisms of recognition, activation and downstream signalling are poorly understood. R proteins of the TIR-NB-LRR (TNL) subclass carry a Toll/Interleukin-1 receptor/Resistance (TIR) protein domain at their N-termini, with homology to cytoplasmic domains of mammalian and *Drosophila* transmembrane immune receptors[6,7]. Examples include the tobacco *N* gene for virus resistance[8], flax *L* and *M* genes for flax rust resistance[9], several *Arabidopsis RPP* genes for downy mildew resistance[10], *Arabidopsis RPS4* (originally defined as conferring recognition of *Pseudomonas syringae* pathovar *pisi* effector AvrRps4)[11] and *Arabidopsis RRS1-R* that confers resistance to *Ralstonia solanacearum* via recognition of effector PopP2 (refs 12,13). The *RRS1-R* allele in accession Nd-1 confers PopP2 recognition, whereas the Col-0 *RRS1-S* allele does not.

RRS1-R (from Ws-2) and *RRS1-S* (from Col-0) are required for AvrRps4 recognition by RPS4, and reciprocally *RPS4* is required for PopP2 recognition by *RRS1-R* in Ws-2 (refs 14,15). *RRS1* and *RPS4* are adjacent, divergently transcribed and function cooperatively for AvrRps4 and PopP2 recognition, and for resistance to the fungus *Colletotrichum higginsianum*[14,15]. NB-LRRs can require other NB-LRRs for function[16]. For example, *RPP2A* and *RPP2B*, two adjacent TNLs in Col-0, are both required for resistance to *Hpa* race Cala2 (ref. 17). Rice *RGA4* and *RGA5* form a NB-LRR pair for recognition of Avr-Pia and Avr1-CO39, two effectors from the fungal pathogen *Magnaporthe oryzae*[18]. Tobacco *N* requires the '*N*-required gene' *NRG1* (ref. 19), and multiple genes of the *ADR1* class are required for function of *RPS2*, *RPP4* and *RPP2* (ref. 20).

In Col-0, mutations in *RRS1* or *RPS4* do not result in complete loss of resistance to *P. syringae* pv *tomato* (*Pst*) strain DC3000 carrying AvrRps4 (refs 14,15,21). Similarly, Ws-2 *rrs1-1* and *rps4-21* mutants show an HR when infiltrated with *Pseudomonas fluorescens* (*Pf*) Pf0-1 (a non-pathogenic *Pseudomonas* strain that carries a type III secretion system) secreting AvrRps4 (refs 22,23). These data suggest that *A. thaliana* Ws-2 and Col-0 carry a *RRS1*- and *RPS4*-Independent AvrRps4 Recognition (*RRIR*) locus.

To dissect AvrRps4-triggered immunity, we positionally cloned the *RRIR* locus. We found another pair of *R* genes, *At5g45050* and *At5g45060,* highly similar to *RRS1*/*RPS4*, which confers RRIR, and named the locus as *RRS1B/RPS4B*. We show using *Agrobacterium*-mediated transient assays in *Nicotiana tabacum* that co-expression of *RRS1B* and *RPS4B* confers recognition of AvrRps4 but not PopP2. The RRS1B and RPS4B proteins associate with each other, as previously reported for RRS1 and RPS4 (ref. 24). Non-authentic R protein associations can also occur between RRS1B and RPS4, and RRS1 and RPS4B, but do not enable effector recognition, suggesting that these R proteins must pair with their appropriate respective partner for function. Although RRS1B/RPS4B does not recognize PopP2, PopP2 still associates *in planta* with RRS1B. TIR domain exchanges between RRS1 and RRS1B, or between RPS4 and RPS4B, do not compromise function. A chimera in which the C-terminal 3 exons of RRS1-R are exchanged for those of RRS1B confers effector-independent HR in combination with RPS4, but not with RPS4B, suggesting integrity of this region is important to prevent defence signalling before effector perception. We finally compare *RRS1*/*RPS4*-like gene pairs in several *Brassicaceae*. These data contribute to understanding TNL-mediated immunity in plants and provide new insights into paired plant immune receptor function and evolution.

Results

***At5g45050* and *At5g45060* co-segregate with the *RRIR* locus.** In Ws-2, the RRIR results in HR as well as disease resistance[23]. This is not due to AvrRps4 recognition by *RRS1* or *RPS4* alone as *Pf* Pf0-1 (AvrRps4) triggers HR not only in Ws-2 *rrs1-1* and *rps4-21* single but also in Ws-2 *rrs1-1*/*rps4-21* double mutants (Fig. 1). No HR was observed in the Ws-2 *eds1-1* mutant, suggesting that RRIR is mediated by a TNL R protein (Fig. 1)[25,26]. Interestingly, *Pf* Pf0-1 (PopP2) does not trigger HR in *rrs1-1* or *rps4-21*, indicating that the RRIR is specific to AvrRps4 (ref. 23). In Col-0, infiltration with either *Pst* DC3000 or *Pf* Pf0 1 producing AvrRps4 does not trigger HR, but disease resistance to *Pst* DC3000 (AvrRps4) is observed (Figs 1 and 2d)[3,23]. *Arabidopsis* accession RLD is susceptible to *Pst* DC3000 (AvrRps4; Supplementary Fig. 1) and was crossed with Ws-2 to map *RPS4* (ref. 11). In addition, RLD does not show HR to *Pf* Pf0-1 (AvrRps4; Fig. 1)[23] indicating absence of RRIR but HR can be observed after *Pf* Pf0-1 (HopA1) infiltration[27]. To positionally clone the *RRIR* locus, we analysed a population generated from a cross between Ws-2 *rps4-21* and RLD (Fig. 1), segregating for HR to *Pf* Pf0-1 (AvrRps4). This enabled us to narrow down a region on chromosome 5 close to *RRS1/RPS4* containing four TNL-encoding genes (Fig. 2a and Supplementary Table 1). Among them, *At5g45050* and *At5g45060* form a pair highly identical to *RRS1*/*RPS4* (Fig. 2b) and were therefore strong candidates for the *RRIR* locus.

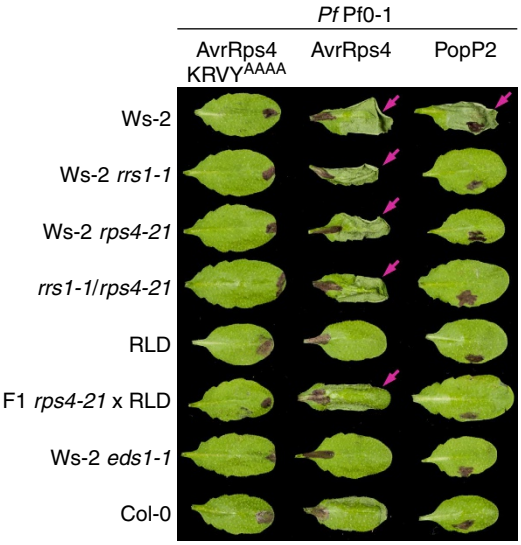

Figure 1 | AvrRps4 but not PopP2 is recognized in the absence of *RRS1* and *RPS4*. Hypersensitive response (HR) assay in different *Arabidopsis* lines using leaf infiltration with *Pseudomonas fluorescens* (*Pf*) Pf0-1 secreting AvrRps4 KRVY^{AAAA}, AvrRps4 or PopP2. Pictures were taken 24 h post infiltration (h.p.i.). Magenta arrows indicate leaves showing HR. This experiment was repeated at least three times with similar results.

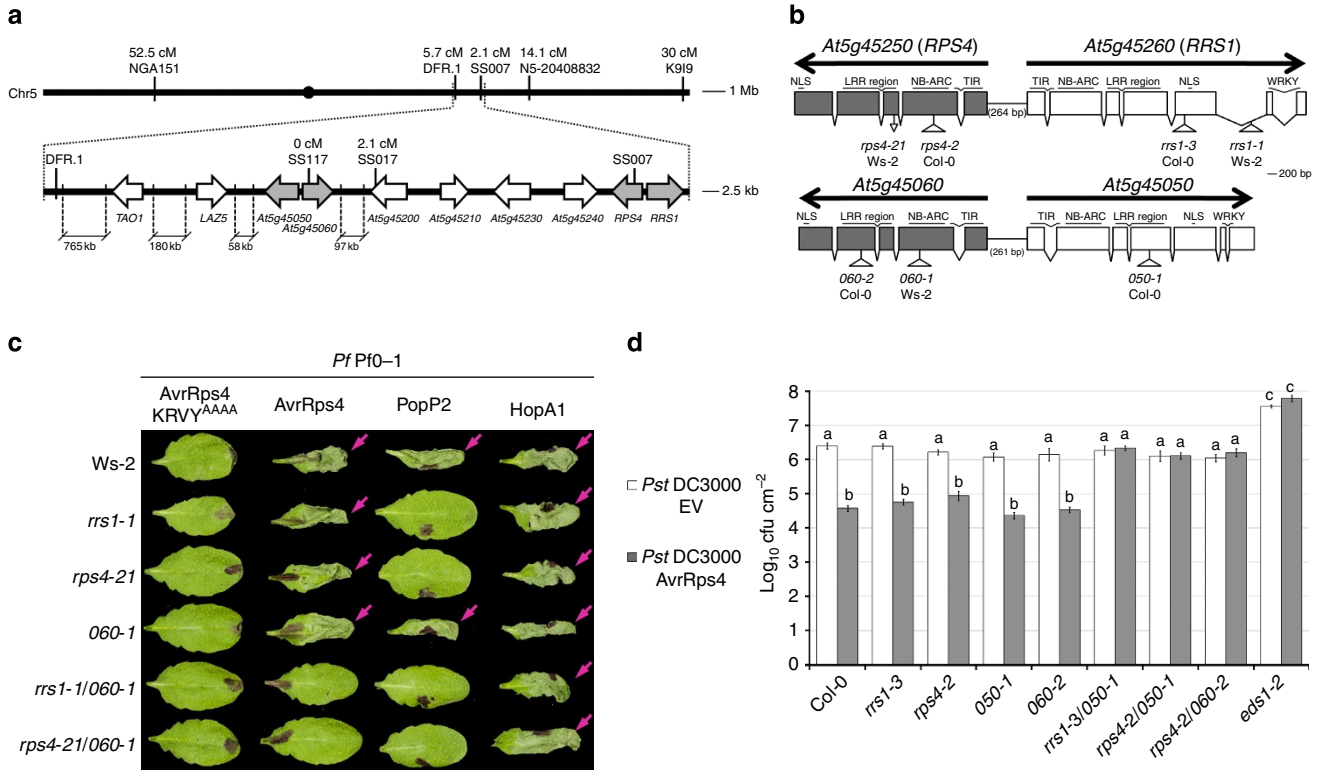

Figure 2 | *At5g45050* and *At5g45060* confer *RRS1/RPS4*-independent AvrRps4 recognition (RRIR). (**a**) Diagram showing the candidate *RRIR* locus (grey arrows) on *Arabidopsis* chromosome 5. Genetic molecular markers used are shown in uppercase letters with corresponding genetic distance (cM) to the *RRIR* locus (based on 48 F2 plants showing no HR to AvrRps4). Arrows represent TNL-encoding genes. Orientation of arrows indicates reading frame direction. The physical distance on the map is indicated in kb or Mb. (**b**) Schematic representation of *RRS1/RPS4* and *At5g45050/At5g45060* gene pairs. Positions of the T-DNA insertion for mutant lines used in this study are indicated by white triangles. *At5g45050* and *At5g45060* are abbreviated as *050* and *060,* respectively. The mutants *rps4-21* (that carries a 5-bp deletion), *rrs1-1* and *rps4-2* were reported previously[14,15,31]. Exons are depicted as boxes, and the different domains are highlighted on the top (APAF1, R proteins and CED4; LRR, leucine-rich repeat; NB-ARC, nucleotide binding, NLS, nuclear localization signal; TIR, Toll/interleukin-1 receptor/R protein; WRKY, WRKY DNA-binding domain). Black arrows indicate the reading frame direction. (**c**) HR assay in Ws-2 and Ws-2 single and double mutants using leaf infiltration with *Pf* Pf0-1 secreting AvrRps4 KRVY^{AAAA}, AvrRps4, PopP2 or HopA1. Pictures were taken 24 h.p.i. Magenta arrows indicate leaves showing HR. (**d**) Bacterial growth of *Pst* DC3000 carrying empty vector (EV) or secreting AvrRps4 in Col-0 WT, single and double mutants. Bacterial growth was measured 3 days post infiltration (d.p.i.). Means ± standard error (s.e.) of four replicates per sample are given. Samples with different letters are statistically different at the 5% confidence level based on Tukey's test. These experiments were repeated at least three times with similar results.

***At5g45050* and *At5g45060* are both required for RRIR**. To investigate whether the *At5g45050/At5g45060* gene pair is the *RRIR* locus, we tested T-DNA insertion mutants *At5g45050-1* (*050-1*) in Col-0, *At5g45060-1* (*060-1*) in Ws-2 and *At5g45060-2* (*060-2*) in Col-0 (Fig. 2b and Supplementary Table 2), for loss of AvrRps4 recognition. These were crossed to *rrs1* or *rps4* mutants (*rrs1-1* in Ws-2; *rrs1-3* in Col-0; *rps4-21* in Ws-2; *rps4-2* in Col-0) in order to recover the following double mutants after PCR screening F2 and F3 progenies: Ws-2 *rps4-21/060-1*, Ws-2 *rrs1-1/060-1*, Col-0 *rrs1-3/050-1*, Col-0 *rps4-2/050-1* and Col-0 *rps4-2/060-2*. Using reverse transcription–PCR (RT–PCR), we confirmed the presence of *RPS4*, *RRS1*, *At5g45060* and *At5g45050* transcripts in Ws-2, Col-0, RLD and *eds1* mutants; we also confirmed the absence of corresponding transcripts in each single and double T-DNA insertion mutants (Supplementary Figs 2 and 3 and Supplementary Table 3). In *rps4-21*, which carries a 5-bp deletion in *RPS4*, the transcript was still detected[15]. We then tested AvrRps4 recognition in these single and double mutants. As expected, Ws-2 *060-1* mutant showed similar HR to Ws-2 after *Pf* Pf0-1 (AvrRps4) infiltration, and retained PopP2 recognition and HR due to the presence of *RRS1/RPS4* (Fig. 2c). The Ws-2 *rrs1-1* and *rps4-21* mutants, on the other hand, showed the loss of HR to PopP2, but maintained HR to AvrRps4 (Fig. 2c). This residual AvrRps4 recognition and HR was completely abolished in Ws-2 *rrs1-1/060-1* or *rps4-21/060-1* double mutants (Fig. 2c), suggesting that *At5g45060* is required for the RRIR in Ws-2. In addition, *rrs1-1/060-1* and *rps4-21/060-1* double mutants showed HR to HopA1 (recognized by the TNL RPS6)[28], suggesting that HR signalling is still effective in these double mutants. None of the mutants or accessions showed HR to *Pf* Pf0-1 carrying a mutated AvrRps4 (AvrRps4 KRVY^{AAAA}), confirming all HR phenotypes resulted from specific effector recognition (Fig. 2c)[29].

To test whether loss of HR to AvrRps4 correlates with loss of disease resistance, we assessed the growth of *Pst* DC3000 (AvrRps4) compared with *Pst* DC3000 (EV) in wild-type (WT) and *Arabidopsis* mutants 3 days post infiltration (d.p.i.). AvrRps4 is recognized in Col-0, restricting *Pst* DC3000 (AvrRps4) growth compared with *Pst* DC3000 (EV), whereas in Col-0 *eds1-2*, *Pst* DC3000 (AvrRps4) grew as much as *Pst* DC3000 (EV) (Fig. 2d). In Col-0 *050-1* and Col-0 *060-2*, with the presence of functional RRS1/RPS4, *Pst* DC3000 (AvrRps4) growth was restricted compared with *Pst* DC3000 (EV) (Fig. 2d). Similarly, restricted growth of *Pst* DC3000 (AvrRps4) was observed in Col-0 *rrs1-3* and Col-0 *rps4-2* due to RRIR (Fig. 2d). However, Col-0 *rrs1-3/050-1*, *rps4-2/050-1* and *rps4-2/060-2* double mutants supported as much *Pst* DC3000 (AvrRps4) growth as *Pst* DC3000 (EV),

indicating the complete loss of AvrRps4 recognition (Fig. 2d). Similar results were shown in Ws-2: *Pst* DC3000 (AvrRps4) grew as well as *Pst* DC3000 (EV) in Ws-2 *rrs1-1/060-1* and *rps4-21/060-1* mutants (Supplementary Fig. 1). This result correlates with the absence of *Pf* Pf0-1 (AvrRps4)-triggered HR in Ws-2 *rrs1-1/060-1* and *rps4-21/060-1* (Fig. 2c). Collectively, these data indicate that both *At5g45050* and *At5g45060* are required for the RRIR in *Arabidopsis* Ws-2 and Col-0. Because of their strong homology to *RRS1* and *RPS4* (Fig. 2b), *At5g45050* and *At5g45060* were designated as *RRS1B* and *RPS4B*, respectively. Surprisingly, neither *rrs1* nor *rps4* mutants showed a significant increase in *Pst* DC3000 (AvrRps4) growth compared with WT Col-0 or Ws-2 (Fig. 2d and Supplementary Fig. 1), in contrast to previous reports[15,21,29], most likely due to different growth conditions.

***RPS4B*^{RLD} premature stop codon causes its loss of function.** The *Arabidopsis* accession RLD is unable to recognize AvrRps4 and carries a non-functional *RPS4*^{RLD} allele (Fig. 1 and Supplementary Fig. 1)[11,30]. We compared RRS1B and RPS4B sequences in RLD and Ws-2 to identify polymorphisms that might account for the loss of function. Compared to RRS1B^{Ws-2}, two non-synonymous substitutions (S586G and I961V) and a deletion of E362 were identified in RRS1B^{RLD} (Supplementary Fig. 4). RPS4B^{RLD} has three non-synonymous substitutions (N264D, C277F and N1053D) and a nucleotide insertion at 3,829 bp, which causes a frame shift and an early stop codon (Supplementary Fig. 5). As a result, RPS4B^{RLD} is missing the C-terminal 63 amino acids (a.a.), including the predicted RPS4B^{Ws-2} nuclear localization signal (NLS). The integrity of RPS4 NLS was reported to be essential for its immune function[31]. Hence, we speculated that the truncation in RPS4B^{RLD} (causing the loss of NLS) rather than the limited polymorphisms in RRS1B^{RLD} could explain the lack of RRIR in RLD. To test the functionality of RPS4B^{RLD} in *Arabidopsis*, we transformed Ws-2 *rps4-21/rps4b-1* with either *RPS4B*^{RLD} or *RPS4B*$^{Ws-2}$. As expected, stable transgenic lines of Ws-2 *rps4-21/rps4b-1*-expressing *RPS4B*^{RLD} did not show HR to *Pf* Pf0-1 (AvrRps4), whereas *rps4-21/rps4b-1*-expressing *RPS4B*$^{Ws-2}$ did (Fig. 3a). This result confirms that *RPS4B*$^{Ws-2}$ is able to complement RRIR in Ws-2 *rps4-21/rps4b-1*, whereas *RPS4B*^{RLD} is non-functional. We then restored the full-length RPS4B^{RLD} protein by removing the adenine insertion at position 3829 in *RPS4B*^{RLD} genomic DNA (gDNA) sequence, and generated RPS4B$^{(\Delta3829)RLD}$ that is almost identical to RPS4B^{Ws-2}. Ws-2 *rps4-21/rps4b-1* stably expressing *RPS4B*$^{(\Delta3829)RLD}$ showed HR to *Pf* Pf0-1 (AvrRps4) at 24 h post infiltration (h.p.i.; Fig. 3a), suggesting the C-terminal 63 a.a. present in RPS4B^{Ws-2} but absent in RPS4B^{RLD} are required for function.

Co-expression of *avrRps4* or *popP2*, together with *RRS1* and *RPS4*, by agro-infiltration in *N. tabacum* leaves results in HR[24]. Using a similar method, we were able to show AvrRps4 recognition by RRS1B/RPS4B in *N. tabacum*. Co-expression of *avrRps4*, but not *GFP*, together with *RRS1B*$^{Ws-2}$ and *RPS4B*$^{Ws-2}$ triggered HR at 5 d.p.i. (Fig. 3b). We then tested AvrRps4 recognition by RRS1B^{RLD}, RPS4B^{RLD} and RPS4B$^{(\Delta3829)RLD}$ using this assay. Consistent with phenotypes observed in *Arabidopsis* RLD and Ws-2 *rps4-21/rps4b-1* complemented lines, co-expression of *RPS4B*^{RLD} with either *RRS1B*^{RLD} or *RRS1B*$^{Ws-2}$ in *N. tabacum* did not show HR to AvrRps4 (Fig. 3b and Supplementary Fig. 6). On the other hand, an AvrRps4-triggered HR was observed when *RRS1B*^{RLD} was co-expressed with either *RPS4B*$^{(\Delta3829)RLD}$ or *RPS4B*$^{Ws-2}$ (Fig. 3b and Supplementary Fig. 6). The stability of each fusion protein used in the transient assay was verified by western blot analysis (Supplementary Fig. 7). These data suggest that RRS1B^{RLD} is functional and that the insertion causing the premature stop codon in RPS4B^{RLD} is responsible for non-functionality and loss of RRIR in the RLD accession.

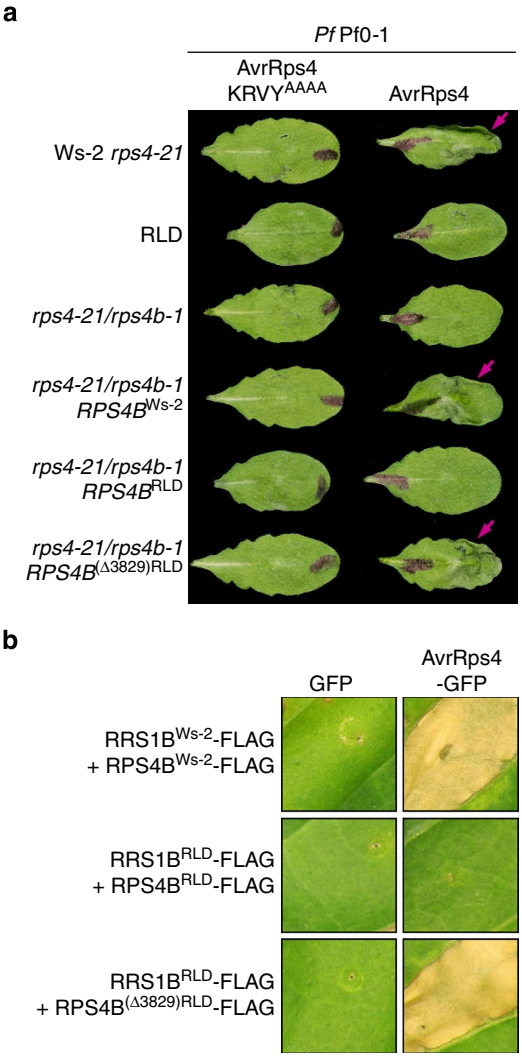

Figure 3 | *RPS4B*^{RLD} carries a mutation responsible for loss of AvrRps4 recognition. (**a**) HR assay using leaf infiltration with *Pf* Pf0-1 secreting AvrRps4 KRVY^{AAAA} or AvrRps4 in Ws-2 *rps4-21*, RLD, Ws-2 *rps4-21/rps4b-1* and stable transgenic lines of Ws-2 *rps4-21/rps4b-1*-expressing *RPS4B*$^{Ws-2}$, *RPS4B*^{RLD} or *RPS4B*$^{(\Delta3829)RLD}$ (under native promoter and terminator). *RPS4B*$^{Ws-2}$ and *RPS4B*^{RLD} were cloned from accession Ws-2 and RLD, respectively. *RPS4B*$^{(\Delta3829)RLD}$ corresponds to *RPS4B*^{RLD} with the WT inserted nucleotide at position 3,829 bp removed, restoring similar coding sequence to Ws-2. Pictures were taken 24 h.p.i. Magenta arrows indicate leaves showing HR. (**b**) HR assay in *N. tabacum* leaves using transient *A. tumefaciens* transformation. Each leaf section was co-infiltrated to express a combination of different *R* genes (shown on the left) together with *GFP* or *avrRps4-GFP*. *RRS1*, *RPS4*, *RRS1B* and *RPS4B* were cloned from Ws-2 or RLD gDNA. Cell death pictures were taken 5 d.p.i. These experiments were repeated at least three times with similar results.

AvrRps4-induced defence genes require either *RPS4* or *RPS4B*. Given two paired *R* genes that provide resistance to one effector, we investigated the quantitative contributions of *RRS1B*/*RPS4B* to AvrRps4-triggered immunity compared with *RRS1*/*RPS4* by measuring defence gene induction using quantitative RT–PCR. Based on previous studies, we selected defence marker genes (*SARD1*, *SID2*, *PAD4* and *EDS5*) that are specifically regulated by

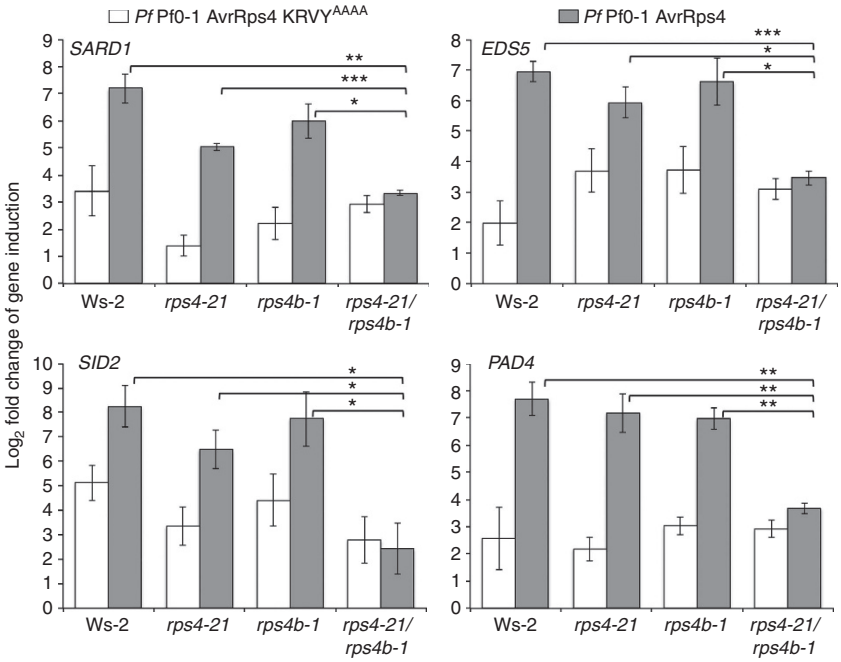

Figure 4 | Loss of *RPS4* and *RPS4B* completely abolishes AvrRps4-triggered defence gene induction in Ws-2. Quantitative RT–PCR showing fold change of *SARD1*, *SID2*, *EDS5* and *PAD4* gene expression. Transcript levels were estimated in leaves of 5-week-old Ws-2, Ws-2 *rps4-21* and *rps4b-1* single and Ws-2 *rps4-21/rps4b-1* double mutants infiltrated with either H_2O, *Pf* Pf0-1 secreting AvrRps4 KRVY^{AAAA} or AvrRps4. RNA was extracted from samples taken at 6 h.p.i. for cDNA synthesis. Results of quantitative RT–PCR for selected defence marker genes were first normalized to *EF1α*, then calculated as $\log_2$-scaled fold change compared with H_2O treatment. Means ± s.e. of three biological replicates per sample are given. Data from individual experiments are shown in Supplementary Fig. 7. Differences that are statistically significant are indicated (Student's *t*-test $^*P \leq 0.05$, $^{**}P \leq 0.01$, $^{***}P \leq 0.001$).

AvrRps4 and PopP2 in a *RRS1/RPS4*-dependent manner at early stages of immunity[27]. Genotypes Ws-2, Ws-2 *rps4-21*, Ws-2 *rps4b-1* and *rps4-21/rps4b-1* were infiltrated with either H_2O, *Pf* Pf0-1-carrying AvrRps4 or AvrRps4 KRVY^{AAAA} mutant. Six hours post infiltration, the fold change of all selected defence marker genes compared with H_2O treatment was consistently more induced in Ws-2, *rps4-21* or *rps4b-1* after infiltration with *Pf* Pf0-1 (AvrRps4) than with *Pf* Pf0-1 (AvrRps4 KRVY^{AAAA}; Fig. 4 and Supplementary Table 4). Assuming that each pair functions independently, this indicates that RRS1B/RPS4B (in *rps4-21*) and RRS1/RPS4 (in *rps4b-1*) were able to activate a similar set of defence genes upon AvrRps4 recognition, and are therefore likely to share downstream signalling mechanisms. In the single knockout mutants tested, there was no consistent pattern of quantitative differences between RRS1/RPS4- and RRS1B/RPS4B-dependent defence genes fold induction triggered by AvrRps4 (Fig. 4 and Supplementary Fig. 8). We also could not observe greater gene induction in Ws-2 compared with the either single mutants. We infer that RRS1/RPS4 and RRS1B/RPS4B independently activate defence genes to a level adequate for resistance in response to AvrRps4. In the *rps4-21/rps4b-1* double mutant fold induction of defence genes triggered by *Pf* Pf0-1 (AvrRps4) is not different to *Pf* Pf0-1 (AvrRps4 KRVY^{AAAA}), but is significantly lower than in AvrRps4-treated Ws-2 or single mutants (Fig. 4). This means AvrRps4-triggered defence genes induction is fully dependent on functional RRS1B/RPS4B and/or RRS1/RPS4, which is consistent with the loss of resistance to *Pst* DC3000 (AvrRps4) observed in the double mutants (Fig. 2d and Supplementary Fig. 1).

RRS1B and RPS4B associate and function together. We have established that there are two *R* gene pairs with ~60% identity that function independently to recognize AvrRps4 (Supplementary Figs 9 and 10). Therefore, we wanted to understand how these R proteins work with their specific pair partners. Genetic evidence of pair specificity was shown in Fig. 2c where the *RRS1B + RPS4* combination in Ws-2 *rrs1-1/rps4b-1* cannot give HR to *Pf* Pf0-1 (AvrRps4). Similarly, the *RRS1 + RPS4B* combination in Col-0 *rps4-2/rrs1b-1* does not give resistance to *Pst* DC3000 (AvrRps4; Fig. 2d). In an *N. tabacum* transient assay, co-expression of *RRS1-R + RPS4B* or *RRS1B + RPS4* combinations did not give HR to either AvrRps4 or PopP2 (Fig. 5a,b and Supplementary Fig. 11). In contrast, *popP2* only triggered HR when co-expressed with *RRS1-R + RPS4*, and *avrRps4*-triggered HR with both *RRS1-R + RPS4* and *RRS1B + RPS4B* (Fig. 5a). This confirms that each R protein requires its cognate pair partner for function.

RRS1 and RPS4 physically associate to form a functional recognition complex *in planta*[24]. Therefore, we tested by co-immunoprecipitation (co-IP) whether RRS1B and RPS4B also associate *in planta*, and if this association is specific to pair partners. Similar to RRS1-GFP and RPS4-FLAG, RRS1B-GFP co-IP with RPS4B-FLAG when transiently co-expressed in *Nicotiana benthamiana* leaves (Fig. 5b lanes 2 and 6, and Supplementary Fig. 12). Interestingly, we also found RRS1B-GFP co-IP with RPS4-FLAG, and RRS1-GFP co-IP with RPS4B-FLAG (Fig. 5b lanes 3 and 5 and Supplementary Fig. 12). However, the intensity of the co-IP signals was notably higher with the appropriate pair partners than with the inappropriate partners. We infer that the complexes formed of inappropriate pairing (for example, *RRS1 + RPS4B* or *RRS1B + RPS4)* are less stable, which could explain their non-functionality. Collectively, similar to RRS1/RPS4, RRS1B/RPS4B associate *in planta* to form a complex before any effector perception, and R protein pair complexes are only functional when formed of the appropriate partners.

RRS1B and RPS4B TIR domains associate *in planta*. TIR domains are considered to play a crucial role in defence activation

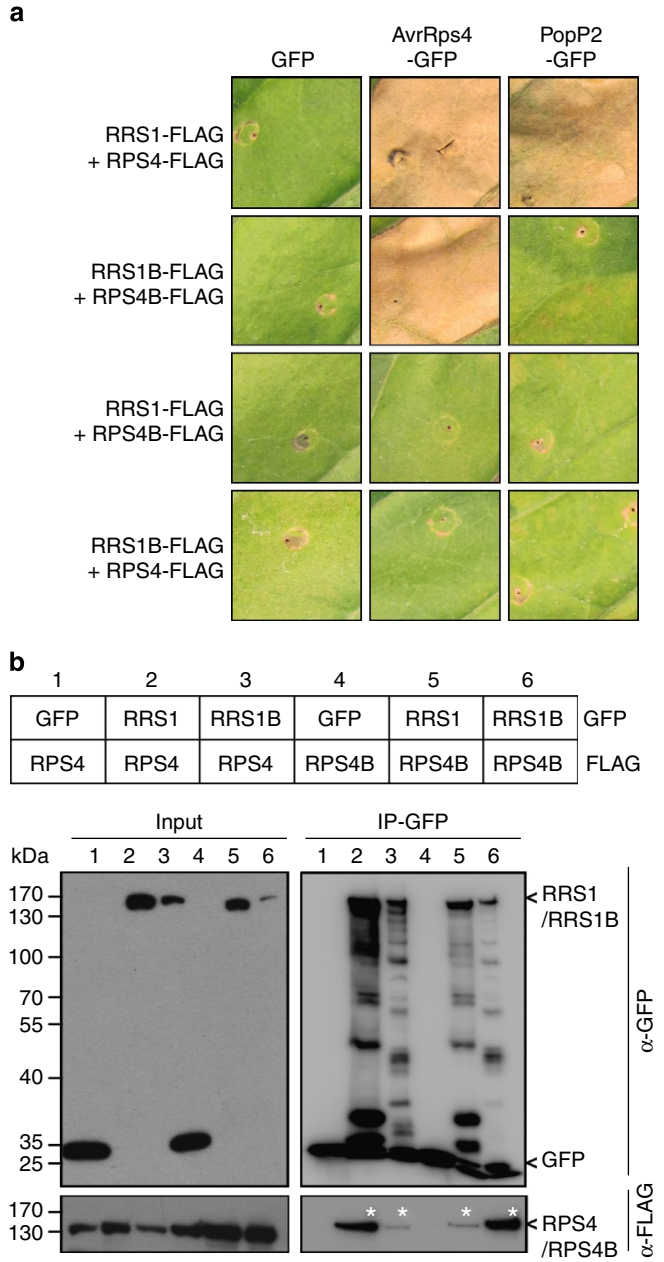

Figure 5 | Corresponding pair partner association *in planta* is required for function. (**a**) HR assay in *N. tabacum* leaves using transient *A. tumefaciens* transformation. Each leaf section was co-infiltrated to express a different combination of *R* genes (shown on the left) together with *GFP, avrRps4-GFP* or *popP2-GFP*. *RRS1, RPS4, RRS1B* and *RPS4B* were cloned from Ws-2 gDNA. Cell death pictures were taken 5 d.p.i. (**b**) Co-immunoprecipitation (co-IP) analysis showing associations within and between RRS1/RPS4 and RRS1B/RPS4B pair proteins. *RRS1, RPS4, RRS1B* and *RPS4B* were fused to either a C-terminal FLAG or GFP tag. The combination of fusion proteins in each sample (C-terminal tag indicated on the right) is listed in the panel with a corresponding number (1–6). Immunoblots show the presence of proteins in total extracts (Input) and after IP with anti-GFP beads (IP-GFP). Asterisks indicate the presence of protein bands after co-IP. These experiments were repeated at least three times with similar results.

as some of them can trigger immune responses when overexpressed alone *in planta*[32–36]. We showed overexpression of RPS4^{TIR} (1–235 a.a.)-triggered cell death in *N. tabacum*, whereas RRS1^{TIR} (1–175 a.a.) did not (Fig. 6a), consistent with previous report[24]. Interestingly, neither RPS4B^{TIR} (1–235 a.a.) nor RRS1B^{TIR} (1–166 a.a.) triggered cell death when overexpressed in *N. tabacum* (Fig. 6a). This implies either polymorphisms in RPS4B^{TIR} compared with RPS4^{TIR} abolish its capacity to activate cell death or that *N. tabacum* lacks a components required for RPS4B^{TIR}-triggered cell death.

Many lines of evidence suggest TIR–TIR interactions are important for TNL function[24,37]. The TIR domains of RRS1 and RPS4 interact in a yeast two hybrid assay and associate *in planta* after co-IP[24]. TIR domains of these proteins are essential for effector recognition and defence activation[24]. In the pre-activation state, the RRS1/RPS4 heterodimer is proposed to be inactive. This correlates with the RRS1^{TIR} suppression of RPS4^{TIR}-triggered cell death when the TIR domains of these two paired R proteins associate (Fig. 6a)[24]. Interestingly, we found that RRS1B^{TIR} can also suppress RPS4^{TIR}-triggered cell death (Fig. 6a), suggesting that TIR domains from different pairs can interact. Therefore, we investigated whether RRS1B^{TIR} and RPS4B^{TIR} can associate with each other *in planta*, and whether they can associate with RPS4^{TIR} and RRS1^{TIR}, respectively, by co-IP. After agro-infiltration in *N. benthamiana,* RRS1B^{TIR}-FLAG co-IP with both RPS4B^{TIR}-GFP and RPS4^{TIR}-GFP; and RPS4B^{TIR}-FLAG co-IP with both RRS1B^{TIR}-GFP and RRS1^{TIR}-GFP (Fig. 6b and Supplementary Fig. 13). This suggests that, similar to full-length proteins, RRS1B^{TIR} and RPS4B^{TIR} can heterodimerize and also associate with RPS4^{TIR} and RRS1^{TIR}, respectively, *in planta*.

TIR swaps between R protein pairs retain function. We next assessed if, despite association of TIR domains between non-paired R proteins, the TIR domains contribute to the specificity of R protein function with each respective pair partner. To answer this question, we constructed chimeras in which RRS1$^{Ws\text{-}2}$ and RRS1B$^{Ws\text{-}2}$ TIR domains were exchanged, and similarly with RPS4$^{Ws\text{-}2}$ and RPS4B$^{Ws\text{-}2}$ TIR domains. We designated the four domains of RRS1 and RPS4 (TIR, NB, LRR and C-Terminal Domain) as 'AAAA' and of RRS1B and RPS4B as 'BBBB', defining TIR domain swaps as RRS1^{BAAA} and RRS1^{ABBB} full-length chimeric proteins (Fig. 6c). These chimeras were tested with WT R proteins for AvrRps4 and PopP2 recognition in *N. tabacum* transient assay. Similar to RRS1^{AAAA} and RPS4^{AAAA}, RRS1^{BAAA} + RPS4^{AAAA} and RRS1^{AAAA} + RPS4^{BAAA} combinations recognized both AvrRps4 and PopP2 (Fig. 6d). On the other hand, similar to RRS1^{BBBB} and RPS4^{BBBB}, RRS1^{ABBB} + RPS4^{BBBB} and RRS1^{BBBB} + RPS4^{ABBB} recognized AvrRps4 only (Fig. 6d). Accumulation of chimeric proteins was confirmed by immunoblot (Supplementary Fig. 14a,b). These results show that exchange of TIR domains from paralogous *R* genes does not compromise AvrRps4 or PopP2 recognition. In addition, the TIR domains do not drive the pair partner specificity for function, therefore other domain–domain interactions must account for the pairing specificity.

We also characterized additional domain swaps between RRS1 and RRS1B, with the breakpoint between the end of exon 4 and the beginning of exon 5. Exons 5, 6 and 7 encode the WRKY domain of these proteins and ~260 amino acids between the LRR domain and the WRKY domain. These swaps were designated as 'AAAB' and 'BBBA', and tested for recognition of AvrRps4 and PopP2 in the presence of either RPS4 or RPS4B. Accumulation of chimeric proteins was confirmed by immunoblot (Supplementary Fig. 14c, d). Neither of the RRS1^{AAAB} and RRS1^{BBBA} chimeras conferred recognition of AvrRps4 or PopP2 (Supplementary Fig. 15). However, RRS1^{AAAB} in combination with RPS4 showed constitutive activity and triggered cell death in the absence of effector, but not in combination with RPS4B (Supplementary Fig. 15). This suggests that integrity and

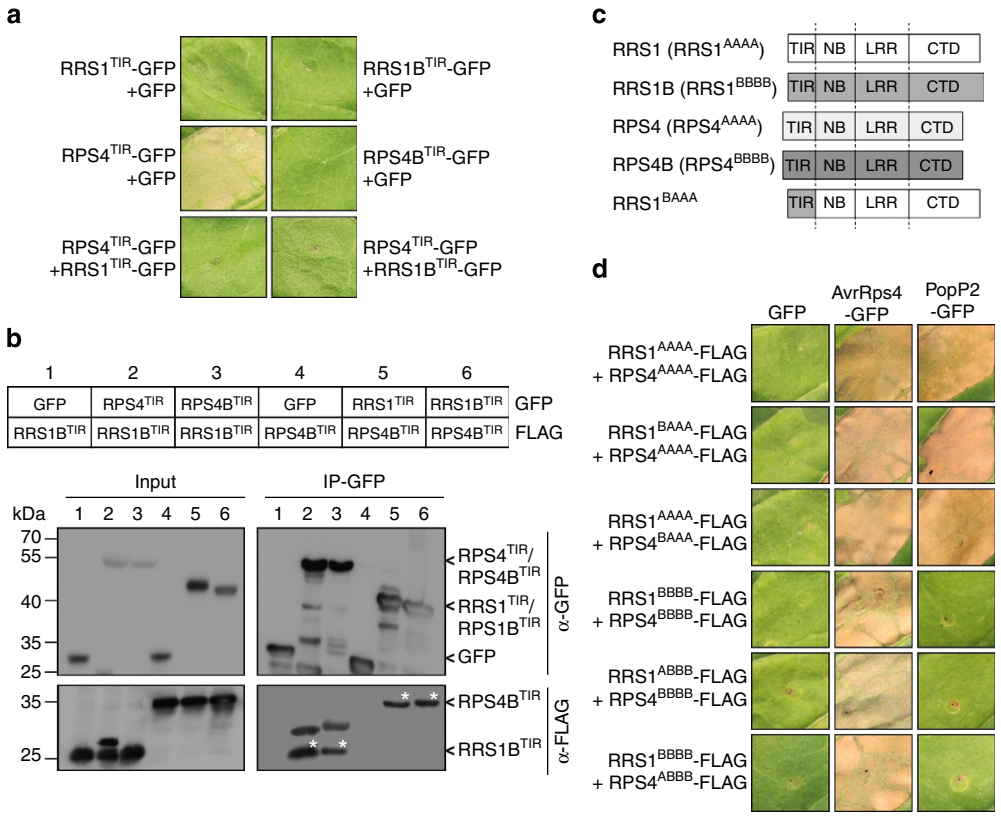

Figure 6 | The TIR domains of RRS1/RPS4 and RRS1B/RPS4B do not confer recognition or association specificity. (**a**) HR assay in *N. tabacum* leaves using *A. tumefaciens*-mediated transient expression of *RRS1, RPS4, RRS1B* and *RPS4B* TIR domains. Each leaf section was co-infiltrated by either single TIR domain with GFP control or by different TIR domain combinations. Cell death pictures were taken 5 d.p.i. (**b**) Co-IP analysis showing association of TIR domains from respective or different pair partners. TIR domains of *RRS1, RPS4, RRS1B* and *RPS4B* were cloned from Ws-2 gDNA and fused to either a C-terminal FLAG or GFP tag. The combination of fusion proteins in each sample (C-terminal tag indicated on the right) is listed in the panel with a corresponding number (1–6). Immunoblots show the presence of proteins in total extracts (Input) and after IP with anti-GFP beads (IP-GFP). Asterisks indicate the presence of protein bands after co-IP. (**c**) Schematic representation of RRS1, RRS1B, RPS4, RPS4B from Ws-2, and a chimera protein $RRS1^{BAAA}$. Each protein was shown with domain structure: RRS1 or RRS1B as TIR-NB-LRR-CTD (C-Terminal Domain)-WRKY; RPS4 or RPS4B as TIR-NB-LRR-CTD. Each domain is indicated with an 'A' or 'B', depending on which pair they belong to: RRS1/RPS4 ('A' pair), RRS1B/RPS4B ('B' pair). (**d**) HR assay in *N. tabacum* leaves using transient *A. tumefaciens* transformation. Each leaf section was co-infiltrated to express a different combination of WT and chimera proteins with TIR domains exchanged between 'A' pair and 'B' pair proteins (shown on the left) together with *GFP, avrRps4-GFP* or *popP2-GFP*. $RRS1^{BAAA}$ and $RRS1^{ABBB}$ were generated by swapping sequences coding for TIR domains between RRS1 and RRS1B. $RPS4^{BAAA}$ and $RPS4^{ABBB}$ were generated similarly. Cell death pictures were taken 5 d.p.i. These experiments were repeated at least three times with similar results.

appropriate interactions in the C-terminal regions of these proteins might be required to prevent effector-independent defence activation.

RRS1B associates with AvrRps4 and PopP2 *in planta*. Recently, it was shown that the RRS1-R/RPS4 R protein complex associates with AvrRps4 and PopP2 *in planta*[24]. RRS1 and PopP2 were also shown to interact in a yeast split-ubiquitin assay[13]. However, this interaction is not sufficient for R protein activation as PopP2 also interacts with RRS1-S^{Col-5} but does not trigger an immune response in Col-5 (ref. 13). We examined whether RRS1B/RPS4B can also associate with AvrRps4 and also PopP2 *in planta* even if RRS1B/RPS4B cannot recognize PopP2. We co-expressed $RRS1^{Ws-2}$*-FLAG* + $RPS4^{Ws-2}$*-FLAG* and $RRS1B^{Ws-2}$*-FLAG* + $RPS4B^{Ws-2}$*-FLAG*, with either *GFP*, *avrRps4-GFP* or *popP2-GFP* in *N. benthamiana*. The GFP protein alone did not co-IP with the RRS1/RPS4 and RRS1B/RPS4B complexes (Supplementary Figs 16 and 17). Similar to RRS1/RPS4 complex, RRS1B/RPS4B complex co-IP with both AvrRps4-GFP and PopP2-GFP (Supplementary Figs 16 and 17). Interestingly, the signal intensity for RRS1/RPS4 was much stronger compared with RRS1B/RPS4B, indicating the RRS1/RPS4 complex has stronger affinity for both effectors than the RRS1B/RPS4B complex. Despite this observation, this result suggests that RRS1B/RPS4B associates *in planta* with AvrRps4 but also with PopP2. However, we cannot exclude that AvrRps4 and PopP2 break the pre-formed R protein heterodimer to associate with each of the partner separately. Considering the high intensity of RRS1 protein bands compared with RPS4 after AvrRps4 and PopP2 IP, we then tested whether RRS1 and RRS1B alone could associate with these effectors. Consistent with Williams *et al.*[24], RRS1 co-IP with both AvrRps4 and PopP2 (Fig. 7 lanes 3 and 5, and Supplementary Fig. 18)[24]. Interestingly, RRS1B also co-IP with both AvrRps4 and PopP2 (Fig. 7 lanes 4 and 6, and Supplementary Fig. 18). Like in complex with their partner, RRS1 showed a stronger association with AvrRps4 and PopP2 than RRS1B. Altogether, this suggests that, similar to RRS1-S/RPS4 (ref. 13), protein–protein association of PopP2 with RRS1B/RPS4B can be detected but this is not sufficient for defence activation.

Pair duplication and gain of WRKY domain in the *Brassicaceae*. To shed some light on the evolution of these tandem paired *R* genes, we examined the genomes of several species related to

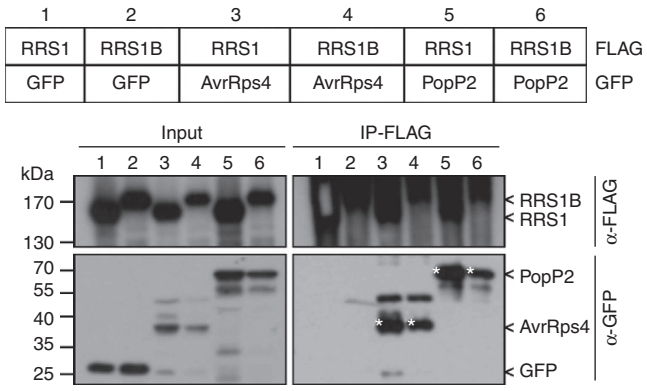

Figure 7 | Similar to RRS1, RRS1B associates with AvrRps4 and PopP2 *in planta*. Co-IP analysis showing association of RRS1 and RRS1B with AvrRps4 and PopP2. *RRS1* and *RRS1B* were cloned from Ws-2 gDNA. The combination of fusion proteins in each sample (C-terminal tag indicated on the right) is listed in the panel with a corresponding number (1 to 6). Immunoblots show the presence of proteins in total extracts (Input) and after IP with anti-FLAG beads (IP-FLAG). Asterisks indicate the presence of protein bands after co-IP.

A. thaliana. Using the nucleotide sequences of each gene from each pair in megablast searches[38], we found that in the genomes of the sister species *Arabidopsis lyrata*[39], and the closely related species *Capsella rubella*[40], there are distinct putatively orthologous pairs matching both the 'A' pair (*RRS1/RPS4*) and 'B' pair (*RRS1B/RPS4B*). In *A. lyrata,* we also found an apparent duplication of the 'B' pair, resulting in a paralogous 'C' pair with a high level of identity to the 'B' pair (Fig. 8b,c). Genome to genome comparison revealed that the regions of the *A. thaliana*, *C. rubella* and *A. lyrata* genomes harbouring the linked pairs were syntenic, with broad conservation of DNA sequence similarity and directionality (Supplementary Fig. 19). Although highly syntenic, the region in *A. lyrata* is expanded in comparison to *A. thaliana* and *C. rubella* (Supplementary Fig. 19). Additionally in *A. lyrata*, we found a divergently transcribed pair of TNL-encoding genes (gene names: *9301337* and *9301336)* with similar identity to both the 'A' and 'B' pairs, which we named *AlRPS4*-like and *AlRRS1*-like, respectively (Fig. 8a–c). The *RRS1*-like gene of this pair, however, lacks the WRKY protein-encoding sequence, which is fused to *RRS1* and *RRS1B*. Inspection of the DNA sequence directly following this *RRS1*-like gene confirmed that this was not due to the presence of an early stop codon. We also examined the genome of the more distant *Arabidopsis* relative *Brassica rapa*[41]. In the *B. rapa* genome, we found no WRKY-fused NB-LRR-encoding genes. A single *B. rapa* gene pair (gene names: *Bra027598* and *Bra027599*) had the highest identity to the *A. thaliana* 'A' and 'B' pairs and is located in a region syntenic to the 'A' and 'B' region on *A. thaliana* chromosome 5 (Fig. 8a–c and Supplementary Fig. 20). This pair lacks a WRKY fusion, and shows the highest nucleotide and protein level identity with *AlRPS4*-like and *AlRRS1*-like. We therefore speculate that these are the ancestors of the 'A', 'B' and 'C' pairs lacking the WRKY fusion. The *B. rapa RRS1*-like gene (*Bra027598*) is fused to another, distantly related, TIR-NB-LRR-encoding gene at its 3′ end, although this may be a genome assembly or gene prediction artefact. Only the *RRS1*-like half was used for the analyses presented. Although their amino-acid sequences have diverged, we found that the DNA sequences of each species' *RRS1* or *RRS1B/C* WRKY domain had the highest nucleotide identity and longest alignment to *AtWRKY35* (selected alignments in Supplementary Fig. 21). These results suggest that a duplication of the ancestral pair fused with the sequence of a *WRKY35*-like gene in the common ancestor of *A. thaliana*, *C. rubella* and *A. lyrata*. Later in this common ancestor, a duplication event produced the 'A' and 'B' pairs. Specifically in the *A. lyrata* lineage, a further duplication of the 'B' pair occurred, resulting in the 'C' pair.

Discussion

This study revealed that *RRS1B/RPS4B*, an *R* gene pair paralogous and closely linked to *RRS1/RPS4,* also recognizes AvrRps4, but not PopP2. In this system, multiple paired R proteins cooperate in a specific manner for the recognition of several effectors from unrelated plant pathogens (Supplementary Fig. 22).

The evolutionary advantage for the plant to carry two *R* gene pairs recognizing the same effector, AvrRps4, is unclear. Conceivably, *RRS1B/RPS4B*, which recognizes AvrRps4, duplicated to create *RRS1-R/RPS4*, recognizing AvrRps4 and PopP2. Although our analyses of the genomes of various relatives of *A. thaliana* could not reveal which of the two pairs is ancestral, we did uncover the probable pre-WRKY fusion ancestor of both pairs, present in *B. rapa* and *A. lyrata*. We also found that distinct orthologous pairs are conserved in the *A. lyrata* and *C. rubella* genomes, suggesting that there is a selective advantage to maintaining both pairs. Indeed, in *A. lyrata* the 'B' pair has further duplicated to produce a closely related 'C' pair. We speculate that the duplication of such *R* gene pairs might reduce the effect of purifying selection and increase the potential for one of the pairs to evolve new or expanded effector recognition capacity[42]. In addition, developing two or more similar recognition systems might enable the plant to maximize protection of an important cellular complex generally targeted by pathogen effectors. However, accession RLD lost both RRS1/RPS4 and RRS1B/RPS4B functions. Conceivably, RLD evolved in an environment not exposed to pathogens recognized by *RRS1/RPS4* and/or *RRS1B/RPS4B*, and mutating these two *R* gene pairs could enhance fitness if there is a cost to resistance. Another hypothesis is that mutating these *R* gene pairs would have avoided a hybrid incompatibility[43]. Indeed, mutations in *RRS1* can cause auto-activity of the RRS1/RPS4 complex leading to growth arrest[44] and this could also be the case for RRS1B/RPS4B.

The appropriate partners of each of RRS1/RPS4 and RRS1B/RPS4B are required for effector-triggered immunity. These proteins form heteromeric complexes in a resting state before effector perception (Supplementary Fig. 22a). In addition, heteromeric complexes can be formed between partners from different pairs before effector recognition. However, such complexes are not functional for AvrRps4 and PopP2 recognition and/or downstream signalling activation. Altogether, this indicates that despite the similarity in motif prediction, TNLs evolved particular inter-molecular specificity for function. The TIR domains are not responsible for this phenomenon, and this specificity must be conferred by domains elsewhere in the R protein. However, we cannot exclude that association between WT proteins and TIR domains from different pairs is the result of overexpression in *N. benthamiana*, which might not occur under native expression. Integrity of NB-LRR protein is an important factor for function. Swapping parts of NB or LRR domains between the Rx and Gpa2 protein disrupt specific intra-molecular interactions and generate auto-active phenotype[45,46]. Similarly, we attempted to define the domains of RRS1-R responsible for PopP2 recognition by domain swaps with RRS1B. Although we did not identify this domain in this study, we were able to show that a combination of the RRS1^{AAAB} chimera with RPS4, but not with RPS4B, resulted in effector-independent HR. We infer that appropriate interactions between multiple domains in the complex are required to create a functional but not auto-active

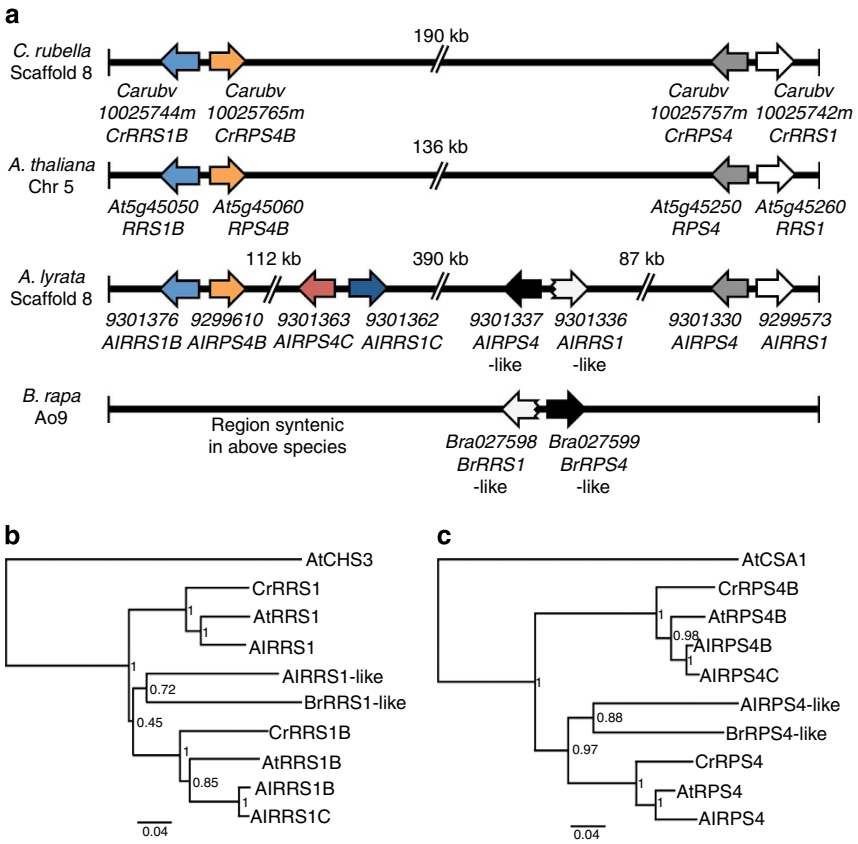

Figure 8 | *RRS1/RPS4*-like *R* gene pair orthologues and progenitors in the *Brassicaceae*. (**a**) Schematic of the *RRS1/RPS4*-like *R* gene pairs in various *Brassicaceae* species. We identified the putative orthologues of *RRS1/RPS4* and *RRS1B/RPS4B* in *A. lyrata* and *C. rubella*. Hypothetical *RRS1*-like genes that lack a WRKY domain are denoted with a broken tailed arrow in *A. lyrata* and *B. rapa*. Synteny was observed in the *RRS1/RPS4* region, although at varying scales (Supplementary Figs 14 and 15). The *AlRRS1C/AlRPS4C* pair is unique to *A. lyrata* and carries a WRKY domain (and is likely a more recent duplication of the B pair). The gene names noted refer to in *C. rubella* and *B. rapa* the Phytozome database, in *A. thaliana* the TAIR database and in *A. lyrata* the NCBI RefSeq database. (**b**) RRS1 orthologues and paralogues cluster into distinct 'A', 'B' and '-like' (non-WRKY) clades. Neighbour-joining tree based on the alignment of the amino-acid sequences of the various RRS1, RRS1-like proteins and a more distantly related outgroup, CHilling Sensitive 3 (CHS3)[64]. The numbers at nodes represent their bootstrap support (% support out of 1,000 bootstraps). The scale bar represents the number of amino-acid substitutions per site. (**c**) RPS4 orthologues and paralogues cluster into distinct 'A', 'B' and '-like' clades. Neighbour-joining tree based on the alignment of the amino-acid sequences of the various RPS4- and RPS4-like proteins and a more distantly related outgroup, Constitutive Shade Avoidance 1 (CSA1)[65]. The numbers at nodes represent their bootstrap support (% support out of 1000 bootstraps). The scale bar represents the number of amino-acid substitutions per site.

complex. Additional domain swap experiments between the two pairs will provide an opportunity for further mechanistic investigation.

Several *TNL*s have been shown to recognize an effector directly and this direct interaction is presumed to trigger R protein activation[13,47–49]. The exact mechanism by which RRS1/RPS4 and RRS1B/RPS4B recognize AvrRps4 and PopP2 has not yet been reported. Although we only showed protein association by co-IP, we can speculate that the potential direct interaction of AvrRps4 with RRS1/RPS4 and RRS1B/RPS4B triggers R protein intra-molecular reconfigurations (and perhaps changes in oligomerization) leading to defence activation (Supplementary Fig. 22b). Such mechanisms could also be suggested for PopP2 recognition but, even if RRS1B/RPS4B associate with PopP2, this association does not trigger immunity. Therefore, an additional molecular event, occurring in the RRS1/RPS4/PopP2 but not in RRS1B/RPS4B/PopP2 complex, might be required (Supplementary Fig. 22c). Both RRS1 and RRS1B carry WRKY domains in their C-termini. WRKY domain-containing proteins play crucial roles in regulating plant defence[50]. If AvrRps4 and PopP2 virulence activities are to target WRKY domain-containing proteins, we could hypothesize that RRS1 and RRS1B, in association with RPS4 and RPS4B, respectively, could behave as decoys for effectors[44,51]. Intriguingly, at the nucleotide level, the WRKY domain of all the *RRS1* orthologues and paralogues shows the highest identity to *WRKY35*, suggesting a common origin. Despite this, the amino-acid sequence of the WRKY domain of RRS1B (WRKY16) is phylogenetically in group IIe of WRKY transcription factors, whereas that of RRS1 (WRKY52) lies in Group III (ref. 52). Conceivably, following duplication, differential adaptive changes occurred in the WRKY domains. If these domains are involved in effector recognition, the two *R* gene pairs may confer recognition of different subsets of WRKY-targeting effectors or effector alleles. Therefore, an important challenge is now to determine the precise role of each RRS1/RPS4 and RRS1B/RPS4B domain, and particularly to identify which of these domain(s) interact with AvrRps4 and PopP2. Also, identification of R protein complex components before and after effector recognition will help us to understand how TNL proteins function to activate plant immunity (Supplementary Fig. 22d,e).

In summary, our data reveal an answer to a long-standing puzzle of how an *Arabidopsis* Col-0 or Ws-2 *rps4* mutant can still activate defence in response to AvrRps4. We show that the RRS1B/RPS4B resembles structurally and functionally the RRS1/RPS4 pair. The RRS1/RPS4 and RRS1B/RPS4B gene pairs will be

the subject of future investigations into the molecular and structural requirements that underpin how pair partner specificity occurs and how an interaction with AvrRps4 or PopP2 is converted into defence activation.

Methods

Plant materials and growth conditions. *A. thaliana*, *N. benthamiana* and *N. tabacum* (cultivar 'Petit Gerard') seeds were sown on compost and vernalized for 7 days (dark, 4 °C). Seedlings and adult plants were grown under controlled conditions: 21–23 °C; 10 h light/14 h dark; 75% humidity for *Arabidopsis*; 21–23 °C; 16 h light/8 h dark; 55% humidity for *Nicotiana sp*. The *Arabidopsis* T-DNA insertion lines used in this study were obtained from the SALK and INRA institutes: *At5g45050-1* (*050-1*) in Col-0 (SALK_001360), *At5g45060-1* (*060-1*) in Ws-2 (FLAG_049F09); *At5g45060-2* (*060-2*) in Col-0 (SALK_063382); *rrs1-3* in Col-0 (SALK_061602); *rps4-2* in Col-0 (SALK_057697). T-DNA insertions were confirmed by PCR using a specific primer of the T-DNA bordure (LBb1.3 primer for SALK lines: 5′-ATTTTGCCGATTTCGGAAC-3′; LB4 primer for FLAG lines: 5′-CGTGTGCCAGGTGCCCACGGAATAGT-3′) and a gene-specific primer (Supplementary Table 2). Lack of expression of the knockout genes was confirmed by RT–PCR (Supplementary Figs 2 and 3 and Supplementary Table 3). Stable transformation using floral dip method[53] was performed on 6- to 7-week-old flowering *Arabidopsis* plants. Genes of interest were amplified from gDNA with specific primers (Supplementary Table 5), cloned into pENTR/D/TOPO and transferred into binary vector *pBGW* (using Gateway System) for *Agrobacterium*-mediated stable transgenic expression *in planta*. From dipped plants, T1 seeds were harvested, sterilized and selected either by spraying soil tray with phosphinothricin, or by growing on GM medium (4.3 g l^{-1} MS salts, 0.1 g l^{-1} myoinositol, 0.59 g l^{-1} MES, 8 g l^{-1} Bacto agar, 1 ml l^{-1} 1,000 × GM vitamin stock, which contains 0.1% thiamine, 0.05% pyridoxine and 0.05% nicotinic acid; pH 5.7) containing appropriate antibiotics. Following similar procedure, T2 and T3 seeds were screened to obtain homozygous stable transgenic lines.

Bacterial infections. For HR assay, *P. fluorescens* (*Pf*) Pf0-1 freshly grown on selective lysogeny broth (LB) agar plates (engineered with type III secretion system)[22], carrying *pVSP61::avrRps4 KRVY*^{AAAA}, *pVSP61::avrRps4, pEDV6::popP2* or *pML123::hopA1* were harvested and resuspended in 10 mM $MgCl_2$ to $OD_{600} = 0.2$ for infiltration. Leaves of 5-week-old *Arabidopsis* plants were hand-infiltrated using 1 ml needless syringe and kept for 20–24 h for symptom (leaf tissue collapse) development. For *in planta* bacterial growth assay, *Pst* DC3000 carrying either *pVSP61* (empty vector) or *pVSP61::avrRps4* were grown on selective LB agar plates and harvested similar to *Pf* Pf0-1 strains. Bacterial suspension in 10 mM $MgCl_2$ were adjusted to $OD_{600} = 0.001$ for infiltration. Leaves of 5-week-old *Arabidopsis* plants were hand-infiltrated and harvested 3 d.p.i. for bacterial count. Infected leaf samples (1 cm^2) were ground in 10 mM $MgCl_2$, serially diluted, spotted on selective LB agar plates and kept at 28 °C for 2 days before counting. Bacterial growing conditions and plasmid mobilization (triparental mating) were performed following published protocols[23].

Quantitative RT–PCR experiments. Leaves of 5-week-old *Arabidopsis* were snap frozen at 6 h.p.i. with water, *Pf* Pf0-1 producing AvrRps4 KRVY^{AAAA} or AvrRps4 for RNA extraction. Total RNAs were extracted using TRI reagent (Sigma), and purified using Qiagen RNeasy columns following the manufacturer's instructions. Integrity of RNAs was assessed by electrophoresis. The complementary DNA was synthesized from 5 µg RNA using SuperScript II Reverse Transcriptase (Invitrogen), and subjected to real-time PCR SYBR Green JumpStart Taq Ready-Mix (Sigma) in the CFX96 Thermal Cycler (Bio-Rad) using specific defence marker gene primers (Supplementary Table 4). Each reaction (~50 ng cDNA per reaction) was performed in triplicates, and the average threshold cycle (Ct) was used to quantify relative gene expression. The relative expression values of defence marker genes were determined using the comparative Ct method ($2^{\Delta Ct}$) with *EF1α* (*At5g60390*) as a reference—normalization. After normalization, the fold change of defence gene induction was calculated on the $\log_2$ scale compared with water (H_2O) infiltrated samples in each genetic background. Statistical analysis was done using Student's *t*-test.

Transient genes expression in *Nicotiana sp*. *Agrobacterium tumefaciens* strain AGL1 carrying various binary constructs were used for transient gene expression and subsequent protein accumulation in *Nicotiana tabacum* (Petit Gerard) or *Nicotiana benthamiana*. Full-length *avrRps4* (1–221 aa) and *popP2* (149–488 a.a.) were cloned and assembled (using pENTR and Gateway System) into binary vector pK7FWG2 (with 35S promoter and C-terminal GFP fusion tag; Supplementary Table 5). Fragments or full-length RRS1, RPS4, RRS1B and RPS4B were amplified from Ws-2 or RLD gDNA for Golden Gate assembly[54] into binary vector *pICH86988* (with 35S promoter and C-terminal FLAG or GFP fusion tag; Supplementary Table 5). TIR domains of RRS1 (1–175 aa), RPS4 (1–235 aa), RRS1B (1–166 aa), RPS4B (1–235 a.a.) were amplified from Ws-2 and assembled similarly into *pICH86988*. Chimera proteins of RRS1 and RRS1B, RPS4 and RPS4B were generated by swapping fragments coding for corresponding domains from either protein (Fig. 6c). To generate RPS4B$^{(\Delta 3829)RLD}$, a nucleotide deletion was performed at 3,829 bp in RPS4B^{RLD} using the QuickChange II XL Site-Directed mutagenesis kit (Agilent). Standard electroporation method was used for transformation of *A. tumefaciens* AGL1. Transformed *A. tumefaciens* were grown in liquid L-medium supplemented with appropriate antibiotics for 24–48 h. Cells were harvested by centrifugation and resuspended at $OD_{600} = 0.4$–0.5 in infiltration medium (10 mM $MgCl_2$, 10 mM MES, pH 5.6). For co-expression, all bacterial suspensions carrying individual constructs were adjusted to $OD_{600} = 0.4$–0.5 in the final mix for infiltration. Five-week-old *N. benthamiana* leaves or *N. tabacum* leaf sections were infiltrated with 1 ml needleless syringe. The infiltrated *N. benthamiana* leaves were taken off at 2 d.p.i. for total protein extraction and co-IP. *N. tabacum* programmed cell death was photographed 5 d.p.i.

Immunoblot analysis and co-IP experiments. Details of immunoblot analysis and co-IP experiments following *Agrobacterium*-mediated transient protein accumulation in *N. benthamiana* leaves were described previously[23]. Protein samples were prepared from *N. benthamiana* leaves 48 h.p.i. with *A. tumefaciens*. One infiltrated leaf was harvested and ground in liquid nitrogen. Proteins were extracted from ground tissues in GTEN buffer (10% glycerol, 100 mM Tris-HCl, pH 7.5, 1 mM EDTA, 150 mM NaCl) supplemented with 5 mM dithiothreitol, 1% (vol/vol) plant protease inhibitor cocktail (Sigma) and 0.2% (vol/vol) Nonidet P-40. Lysates were centrifuged 15 min at 20,000 *g* at 4 °C and aliquots of filtered supernatants were used as input samples. Immunoprecipitations were conducted on 1.5 ml of filtered extract incubated for 2 h at 4 °C under gentle agitation in the presence of 20 µl anti-FLAG M2 affinity Gel (A2220 Sigma-Aldrich) or GFP-Trap_A (gtm-20 ChromoTek). Antibody-coupled agarose beads were collected and washed three times in GTEN buffer, resuspended in 3 × SDS-loading buffer and denatured at 96 °C for 10 min. Proteins were separated by SDS–PAGE and analysed by immunoblotting using anti-FLAG M2-Peroxidase (HRP) (A8592 Sigma) or anti-GFP(B-2) HRP (sc-9996 Santa Cruz Biotechnology). We used 1/10,000 dilution of 200 µg ml^{-1} anti-FLAG and anti-GFP antibodies in 5% non-fat milk.

***RRIR* mapping.** To positionally clone the *RRIR* locus, a segregating population was generated by crossing Ws-2 *rps4-21* with RLD. The Ws-2 *rps4-21* × RLD F1 progeny showed HR to *Pf* Pf0-1 (AvrRps4), although variation in HR intensity was observed compared with the Ws-2 *rps4-21* parent (Fig. 1). This observation suggested a semi-dominance of the RRIR-conferring locus from Ws-2; this weak phenotype was designated 'hr' in contrast to the 'HR' of Ws-2 *rps4-21*. The F2 progeny derived from F1 was then phenotyped (for the presence or absence of HR to *Pf* Pf0-1 (AvrRps4)) and genotyped to map the *RRIR* locus (Fig. 2a and Supplementary Table 1). After infiltration of 48 F2 plants with *Pf* Pf0-1 (AvrRps4), an approximate 1:2:1 ratio (8 (HR):28 (hr):12 (no HR); $\chi^2 = 2$, $P = 0.572$) was observed. This segregation suggested that the RRIR was associated with a single semi-dominant locus. To confirm the ratio observed in F2, we tested the HR phenotype segregation in 8 F3 plants derived from each of the 48 individual F2. By classifying the F3 families (F2:3) into those that showed HR, and those non-segregating for the absence of HR, a 3:1 ratio was observed (37 F2:3 with (HR): 11 F2:3 (no HR); $\chi^2 = 0.111$, $P = 0.945$). This confirmed the presence of a single locus for the RRIR. To map the *RRIR* locus, we obtained and tested a total of 48 F2 individuals that did not segregate for the absence of *Pf* Pf0-1 (AvrRps4)-triggered HR in F3. As AvrRps4 recognition segregates 3:1 in a Ws-2 × RLD cross[11], RRIR is likely to be conferred by a locus that is closely linked to *RRS1*/*RPS4*. Therefore, we focused the mapping on the lower arm of the chromosome 5 (Fig. 2a), around *RPS4*, where all tested loci were homozygous for an RLD genotype in the 48 F2 individuals. Consistent with our hypothesis, markers SS007 (designed on *RPS4*) and SS017 mapped 2.1 cM (2 recombinants out of 48 F2 plants tested) from the *RRIR* locus confirming that *RRIR* and *RPS4* loci were linked but distinct. The markers DFR.1 and N5-20408832 mapped, respectively, 5.7 cM (5 recombinants out of 44 F2 plants tested) and 14.1 cM (13 recombinants out of 46 F2 plants tested) from *RRIR*. The two recombinants (that is, two chromosomes heterozygous for Ws-2 genotype at the marker position) identified with SS017 were also recombinants at the N5-20408832 marker. Interestingly, no recombinants were similarly identified by DFR.1 and SS017 (Fig. 2a). Thus, we concluded that the *RRIR* locus resided between DFR.1 and SS017. In this region, only four TNL-encoding genes are predicted in Col-0 (*TAO1*, *LAZ5*, *At5g45050* and *At5g45060*; Fig. 2a)[55]. We focused on TNL-encoding genes for *RRIR* as AvrRps4-dependent recognition in Ws-2 is *EDS1* dependent[25]. The SS117 marker was designed onto *At5g45060*, a TNL divergently transcribed from *At5g45050*. SS117 co-segregated with the *RRIR* locus (0 recombinants out of 48 F2 plants tested; Fig. 2a). *TAO1* contributes to disease resistance against *Pst* DC3000 carrying AvrB in *Arabidopsis*[56] and *LAZ5* is required for the lesion mimic mutant *acd11* (ref. 57). *At5g45050* and *At5g45060* were hitherto uncharacterized. Interestingly, like *RRS1* and *RPS4*, *At5g45050* and *At5g45060* are divergently transcribed and in a head-to-head configuration. The *RRS1*/*RPS4* and *At5g45050*/*At5g45060* pairs share similar exon/intron architecture (Fig. 2b). At5g45050 and At5g45060 are the closest homologues of RRS1 and RPS4, respectively, within the predicted TNL proteins (with 58% and 64% of identity, respectively)[55].

Analysis of *RRS1/RPS4*-like pairs in *Brassicaceae*. We used nucleotide–nucleotide BLAST 2.2.29 + [58], specifically the megablast algorithm[38], to search

the predicted coding sequence databases from *A. lyrata*[39], *C. rubella*[40] and *B. rapa*[41] with the *A. thaliana* Col-0-coding sequences of *RRS1, RPS4, RRS1B* and *RPS4B*. Following the identification of putatively orthologous genes, MUSCLE[59] and CLUSTAL W[60] nucleotide and protein sequence alignments were used to generate phylogenetic trees using the Neighbour-Joining and Maximum Likelihood (Tamura-Nei model) methods, each with 1,000 bootstraps. These analyses were carried out within the MEGA 6 suite[61]. Note that the trees presented in Fig. 8 were constructed with CLUSTALW protein alignments and the Neighbour-Joining method and were consistent with the trees generated using the other methods. FigTree v1.4 (http://tree.bio.ed.ac.uk/software/figtree/) was used to prepare the trees for publication. To determine the closest WRKY domain nucleotide sequence to the various *RRS1* WRKY domain sequences, a database of all WRKY family genes in *A. thaliana* was searched using nucleotide–nucleotide megablast. Alignment of the nucleotide sequences of *AtWRKY35* and *RRS1* and *RRS1B* was accomplished using the EMBOSS MATCHER online tool[62]. To establish genome–genome synteny, the nucleotide sequences of the genomic regions harbouring the genes of interest were extracted and queried against each other using megablast. The tabular (output format 6) results were then loaded into the Artemis Genome Comparison Tool[63], which was used to visualize and check for synteny across the various *Brassicaceae RRS1/RPS4*-encoding regions.

References

1. Dodds, P. N. & Rathjen, J. P. Plant immunity: towards an integrated view of plant-pathogen interactions. *Nat. Rev. Genet.* **11,** 539–548 (2010).
2. Jones, J. D. & Dangl, J. L. The plant immune system. *Nature* **444,** 323–329 (2006).
3. Gassmann, W. Natural variation in the Arabidopsis response to the avirulence gene hopPsyA uncouples the hypersensitive response from disease resistance. *Mol. Plant Microbe Interact.* **18,** 1054–1060 (2005).
4. Inohara, N., Chamaillard, M., McDonald, C. & Nunez, G. NOD-LRR proteins: role in host–microbial interactions and inflammatory disease. *Annu. Rev. Biochem.* **74,** 355–383 (2005).
5. Lukasik, E. & Takken, F. L. W. STANDing strong, resistance proteins instigators of plant defence. *Curr. Opin. Plant Biol.* **12,** 427–436 (2009).
6. Uematsu, S. & Akira, S. [Toll-like receptor and innate immunity]. *Seikagaku* **79,** 769–776 (2007).
7. Burch-Smith, T. M. & Dinesh-Kumar, S. P. The functions of plant TIR domains. *Sci. STKE* **2007,** pe46 (2007).
8. Whitham, S. *et al.* The product of the tobacco mosaic virus resistance gene *N*: similarity to TolI and the interleukin-1 receptor. *Cell* **78,** 1011–1115 (1994).
9. Ellis, J. G., Dodds, P. N. & Lawrence, G. J. Flax rust resistance gene specificity is based on direct resistance-avirulence protein interactions. *Annu. Rev. Phytopathol.* **45,** 289–306 (2007).
10. Nemri, A. *et al.* Genome-wide survey of Arabidopsis natural variation in downy mildew resistance using combined association and linkage mapping. *Proc. Natl Acad. Sci. USA* **107,** 10302–10307 (2010).
11. Hinsch, M. & Staskawicz, B. Identification of a new Arabidopsis disease resistance locus, RPs4, and cloning of the corresponding avirulence gene, avrRps4, from Pseudomonas syringae pv. pisi. *Mol. Plant -Microbe Interact.* **9,** 55–61 (1996).
12. Deslandes, L. *et al.* Genetic characterization of RRS1, a recessive locus in Arabidopsis thaliana that confers resistance to the bacterial soilborne pathogen Ralstonia solanacearum. *Mol. Plant Microbe Interact.* **11,** 659–667 (1998).
13. Deslandes, L. *et al.* Physical interaction between RRS1-R, a protein conferring resistance to bacterial wilt, and PopP2, a type III effector targeted to the plant nucleus. *Proc. Natl Acad. Sci. USA* **100,** 8024–8029 (2003).
14. Birker, D. *et al.* A locus conferring resistance to Colletotrichum higginsianum is shared by four geographically distinct Arabidopsis accessions. *Plant J.* **60,** 602–613 (2009).
15. Narusaka, M. *et al.* RRS1 and RPS4 provide a dual Resistance-gene system against fungal and bacterial pathogens. *Plant J.* **60,** 218–226 (2009).
16. Eitas, T. K. & Dangl, J. L. NB-LRR proteins: pairs, pieces, perception, partners, and pathways. *Curr. Opin. Plant Biol.* **13,** 472–477 (2010).
17. Sinapidou, E. *et al.* Two TIR:NB:LRR genes are required to specify resistance to Peronospora parasitica isolate Cala2 in Arabidopsis. *Plant J.* **38,** 898–909 (2004).
18. Cesari, S. *et al.* The Rice Resistance Protein Pair RGA4/RGA5 Recognizes the Magnaporthe oryzae Effectors AVR-Pia and AVR1-CO39 by Direct Binding. *Plant Cell* **25,** 1463–1481 (2013).
19. Peart, J. R., Mestre, P., Lu, R., Malcuit, I. & Baulcombe, D. C. NRG1, a CC-NB-LRR protein, together with N, a TIR-NB-LRR protein, mediates resistance against tobacco mosaic virus. *Curr. Biol.* **15,** 968–973 (2005).
20. Bonardi, V. *et al.* Expanded functions for a family of plant intracellular immune receptors beyond specific recognition of pathogen effectors. *Proc. Natl Acad. Sci. USA* **108,** 16463–16468 (2011).
21. Kim, S. H. *et al.* The *Arabidopsis* resistance-like gene SNC1 is activated by mutations in SRFR1 and contributes to resistance to the bacterial effector AvrRps4. *PLoS Pathog.* **6,** e1001172 (2010).
22. Thomas, W. J., Thireault, C. A., Kimbrel, J. A. & Chang, J. H. Recombineering and stable integration of the Pseudomonas syringae pv. syringae 61 hrp/hrc cluster into the genome of the soil bacterium Pseudomonas fluorescens Pf0-1. *Plant J.* **60,** 919–928 (2009).
23. Sohn, K. H., Hughes, R. K., Piquerez, S. J., Jones, J. D. & Banfield, M. J. Distinct regions of the Pseudomonas syringae coiled-coil effector AvrRps4 are required for activation of immunity. *Proc. Natl Acad. Sci. USA* **109,** 16371–16376 (2012).
24. Williams, S. J. *et al.* Structural basis for assembly and function of a heterodimeric plant immune receptor. *Science* **344,** 299–303 (2014).
25. Aarts, N. *et al.* Different requirements for EDS1 and NDR1 by disease resistance genes define at least two R gene-mediated signaling pathways in Arabidopsis. *Proc. Natl Acad. Sci. USA* **95,** 10306–10311 (1998).
26. Liu, Y., Schiff, M., Marathe, R. & Dinesh-Kumar, S. P. Tobacco Rar1, EDS1 and NPR1/NIM1 like genes are required for N-mediated resistance to tobacco mosaic virus. *Plant J.* **30,** 415–429 (2002).
27. Sohn, K. H. *et al.* The nuclear immune receptor RPS4 is required for RRS1SLH1-dependent constitutive defense activation in *Arabidopsis thaliana*. *PLoS Genet.* **10,** e1004655 (2014).
28. Kim, S. H., Kwon, S. I., Saha, D., Anyanwu, N. C. & Gassmann, W. Resistance to the Pseudomonas syringae effector HopA1 is governed by the TIR-NBS-LRR protein RPS6 and is enhanced by mutations in SRFR1. *Plant Physiol.* **150,** 1723–1732 (2009).
29. Sohn, K. H., Zhang, Y. & Jones, J. D. The *Pseudomonas syringae* effector protein, AvrRPS4, requires in planta processing and the KRVY domain to function. *Plant J.* **57,** 1079–1091 (2009).
30. Gassmann, W., Hinsch, M. E. & Staskawicz, B. J. The Arabidopsis RPS4 bacterial-resistance gene is a member of the TIR-NBS-LRR family of disease-resistance genes. *Plant J.* **20,** 265–277 (1999).
31. Wirthmueller, L., Zhang, Y., Jones, J. D. & Parker, J. E. Nuclear accumulation of the Arabidopsis immune receptor RPS4 is necessary for triggering EDS1-dependent defense. *Curr. Biol.* **17,** 2023–2029 (2007).
32. Maekawa, T. *et al.* Coiled-coil domain-dependent homodimerization of intracellular barley immune receptors defines a minimal functional module for triggering cell death. *Cell. Host. Microbe.* **9,** 187–199 (2011).
33. Collier, S. M., Hamel, L. P. & Moffett, P. Cell death mediated by the N-terminal domains of a unique and highly conserved class of NB-LRR protein. *Mol. Plant Microbe Int.* **24,** 918–931 (2011).
34. Frost, D. *et al.* Tobacco transgenic for the flax rust resistance gene L expresses allele-specific activation of defense responses. *Mol. Plant Microbe Interact.* **17,** 224–232 (2004).
35. Weaver, M. L., Swiderski, M. R., Li, Y. & Jones, J. D. The *Arabidopsis thaliana* TIR-NB-LRR R-protein, RPP1A; protein localization and constitutive activation of defence by truncated alleles in tobacco and Arabidopsis. *Plant J.* **47,** 829–840 (2006).
36. Swiderski, M. R., Birker, D. & Jones, J. D. The TIR domain of TIR-NB-LRR resistance proteins is a signaling domain involved in cell death induction. *Mol. Plant Microbe Interact.* **22,** 157–165 (2009).
37. Bernoux, M. *et al.* Structural and functional analysis of a plant resistance protein TIR domain reveals interfaces for self-association, signaling, and autoregulation. *Cell Host Microbe* **9,** 200–211 (2011).
38. Zhang, Z., Schwartz, S., Wagner, L. & Miller, W. A greedy algorithm for aligning DNA sequences. *J. Computat. Biol* **7,** 203–214 (2000).
39. Hu, T. T. *et al.* The *Arabidopsis lyrata* genome sequence and the basis of rapid genome size change. *Nature Genet.* **43,** 476–481 (2011).
40. Slotte, T. *et al.* The Capsella rubella genome and the genomic consequences of rapid mating system evolution. *Nature Genet.* **45,** 831–835 (2013).
41. Wang, X. *et al.* The genome of the mesopolyploid crop species Brassica rapa. *Nature Genet.* **43,** 1035–1039 (2011).
42. Ohno, S. Evolution by Gene Duplication Springer (1970).
43. Bomblies, K. & Weigel, D. Hybrid necrosis: autoimmunity as a potential gene-flow barrier in plant species. *Nat. Rev. Genet.* **8,** 382–393 (2007).
44. Noutoshi, Y. *et al.* A single amino acid insertion in the WRKY domain of the Arabidopsis TIR-NBS-LRR-WRKY-type disease resistance protein SLH1 (sensitive to low humidity 1) causes activation of defense responses and hypersensitive cell death. *Plant J.* **43,** 873–888 (2005).
45. Rairdan, G. J. & Moffett, P. Distinct domains in the ARC region of the potato resistance protein Rx mediate LRR binding and inhibition of activation. *Plant Cell* **18,** 2082–2093 (2006).
46. Slootweg, E. J. *et al.* Structural determinants at the interface of the ARC2 and LRR domains control the activation of the NB-LRR plant immune receptors Rx1 and Gpa2. *Plant Physiol.* **162,** 1510–1528 (2013).
47. Dodds, P. N. *et al.* Direct protein interaction underlies gene-for-gene specificity and coevolution of the flax resistance genes and flax rust avirulence genes. *Proc. Natl Acad. Sci. USA* **103,** 8888–8893 (2006).
48. Krasileva, K. V., Dahlbeck, D. & Staskawicz, B. J. Activation of an Arabidopsis resistance protein is specified by the in planta association of its leucine-rich repeat domain with the cognate oomycete effector. *Plant Cell* **22,** 2444–2458 (2010).

49. Ravensdale, M. *et al.* Intramolecular interaction influences binding of the Flax L5 and L6 resistance proteins to their AvrL567 ligands. *PLoS Pathog.* **8,** e1003004 (2012).
50. Journot-Catalino, N., Somssich, I. E., Roby, D. & Kroj, T. The transcription factors WRKY11 and WRKY17 act as negative regulators of basal resistance in Arabidopsis thaliana. *Plant Cell* **18,** 3289–3302 (2006).
51. van der Hoorn, R. A. & Kamoun, S. From guard to decoy: a new model for perception of plant pathogen effectors. *Plant Cell* **20,** 2009–2017 (2008).
52. Eulgem, T., Rushton, P. J., Robatzek, S. & Somssich, I. E. The WRKY superfamily of plant transcription factors. *Trends Plant Sci.* **5,** 199–206 (2000).
53. Clough, S. J. & Bent, A. F. Floral dip: a simplified method for Agrobacterium-mediated transformation of *Arabidopsis thaliana*. *Plant J.* **16,** 735–743 (1998).
54. Engler, C., Kandzia, R. & Marillonnet, S. A one pot, one step, precision cloning method with high throughput capability. *PLoS ONE* **3,** e3647 (2008).
55. Meyers, B. C. Genome-Wide Analysis of NBS-LRR-encoding genes in arabidopsis. *Plant Cell* **15,** 809–834 (2003).
56. Eitas, T. K., Nimchuk, Z. L. & Dangl, J. L. Arabidopsis TAO1 is a TIR-NB-LRR protein that contributes to disease resistance induced by the *Pseudomonas syringae* effector AvrB. *Proc. Natl Acad. Sci. USA* **105,** 6475–6480 (2008).
57. Palma, K. *et al.* Autoimmunity in Arabidopsis acd11 is mediated by epigenetic regulation of an immune receptor. *PLoS Pathog.* **6,** e1001137 (2010).
58. Altschul, S. F., Gish, W., Miller, W., Myers, E. W. & Lipman, D. J. Basic local alignment search tool. *J. Mol. Biol.* **215,** 403–410 (1990).
59. Edgar, R. C. MUSCLE: multiple sequence alignment with high accuracy and high throughput. *Nucleic Acids Res.* **32,** 1792–1797 (2004).
60. Thompson, J. D., Higgins, D. G. & Gibson, T. J. CLUSTAL W: improving the sensitivity of progressive multiple sequence alignment through sequence weighting, position-specific gap penalties and weight matrix choice. *Nucleic Acids Res.* **22,** 4673–4680 (1994).
61. Tamura, K., Stecher, G., Peterson, D., Filipski, A. & Kumar, S. MEGA6: molecular evolutionary genetics analysis version 6.0. *Mol. Biol. Evol.* **30,** 2725–2729 (2013).
62. Rice, P., Longden, I. & Bleasby, A. EMBOSS: the European molecular biology open software suite. *Trends Genet.* **16,** 276–277 (2000).
63. Carver, T. J. *et al.* ACT: the artemis comparison tool. *Bioinformatics* **21,** 3422–3423 (2005).
64. Yang, H. *et al.* A mutant CHS3 protein with TIR-NB-LRR-LIM domains modulates growth, cell death and freezing tolerance in a temperature-dependent manner in Arabidopsis. *Plant J.* **63,** 283–296 (2010).
65. Faigon-Soverna, A. *et al.* A constitutive shade-avoidance mutant implicates TIR-NBS-LRR proteins in Arabidopsis photomorphogenic development. *Plant Cell* **18,** 2919–2928 (2006).

Acknowledgements

We thank Sylvestre Marillonnet for providing Golden Gate vectors and James Alfano for providing *pML123::hopA1* construct. P.F.S. was supported by the EC FP7-PEOPLE-2011-Intra-European Fellowships Marie Sktodowska-Curie actions (299621); K.H.S. was supported by the Rural Development Administration (Republic of Korea) Woo Jang Chun Project (PJ007850201006). We thank the horticultural services at John Innes Centre for their important contribution and assistance. We particularly thank Nick Pullen, Dan MacLean, Sophie Piquerez, Cécile Segonzac, Ghanasyam Rallapalli, Léo Mongendre and all members of the Jones laboratory for their excellent support and feedback on the manuscript.

Author contributions

S.B.S., J.D.G.J. and K.H.S. designed experiments and analysed the data. S.B.S. carried out the map-based cloning and gene cloning for transient assay. S.B.S. generated and analysed *Arabidopsis* knockout mutants and complemented lines. S.B.S. and Y.M. performed the agro-infiltration assays and the related biochemistry. Y.M. carried out the quantitative PCR test and statistical analysis. O.J.F. developed the evolutionary aspect of *RRS1*/*RPS4*-like paired *R* genes. S.B.S., Y.M. and O.J.F. worked under the supervision and general assistance of P.F.S. S.B.S., Y.M., O.J.F. and J.D.G.J. wrote the manuscript. The project initiation and supervision was carried out by J.D.G.J. with general assistance of K.H.S.

Additional information

Supplementary Information accompanies this paper at http://www.nature.com/naturecommunications

Competing financial interests: The authors declare no competing financial interests.

Reprints and permission information is available online at http://npg.nature.com/reprintsandpermissions/

How to cite this article: Saucet, S. B. *et al.* Two linked pairs of *Arabidopsis TNL* resistance genes independently confer recognition of bacterial effector AvrRps4. *Nat. Commun.* 6:6338 doi: 10.1038/ncomms7338 (2015).